Fermilab-Pub-08/294-E

A search for the standard model Higgs boson in the missing energy and acoplanar b-jet topology at $\sqrt{s} = 1.96$ TeV

V.M. Abazov[36], B. Abbott[75], M. Abolins[65], B.S. Acharya[29], M. Adams[51], T. Adams[49], E. Aguilo[6], M. Ahsan[59], G.D. Alexeev[36], G. Alkhazov[40], A. Alton[64,a], G. Alverson[63], G.A. Alves[2], M. Anastasoaie[35], L.S. Ancu[35], T. Andeen[53], B. Andrieu[17], M.S. Anzelc[53], M. Aoki[50], Y. Arnoud[14], M. Arov[60], M. Arthaud[18], A. Askew[49], B. Åsman[41], A.C.S. Assis Jesus[3], O. Atramentov[49], C. Avila[8], F. Badaud[13], L. Bagby[50], B. Baldin[50], D.V. Bandurin[59], P. Banerjee[29], S. Banerjee[29], E. Barberis[63], A.-F. Barfuss[15], P. Bargassa[80], P. Baringer[58], J. Barreto[2], J.F. Bartlett[50], U. Bassler[18], D. Bauer[43], S. Beale[6], A. Bean[58], M. Begalli[3], M. Begel[73], C. Belanger-Champagne[41], L. Bellantoni[50], A. Bellavance[50], J.A. Benitez[65], S.B. Beri[27], G. Bernardi[17], R. Bernhard[23], I. Bertram[42], M. Besançon[18], R. Beuselinck[43], V.A. Bezzubov[39], P.C. Bhat[50], V. Bhatnagar[27], C. Biscarat[20], G. Blazey[52], F. Blekman[43], S. Blessing[49], K. Bloom[67], A. Boehnlein[50], D. Boline[62], T.A. Bolton[59], E.E. Boos[38], G. Borissov[42], T. Bose[77], A. Brandt[78], R. Brock[65], G. Brooijmans[70], A. Bross[50], D. Brown[81], X.B. Bu[7], N.J. Buchanan[49], D. Buchholz[53], M. Buehler[81], V. Buescher[22], V. Bunichev[38], S. Burdin[42,b], T.H. Burnett[82], C.P. Buszello[43], J.M. Butler[62], P. Calfayan[25], S. Calvet[16], J. Cammin[71], E. Carrera[49], W. Carvalho[3], B.C.K. Casey[50], H. Castilla-Valdez[33], S. Chakrabarti[18], D. Chakraborty[52], K.M. Chan[55], A. Chandra[48], E. Cheu[45], F. Chevallier[14], D.K. Cho[62], S. Choi[32], B. Choudhary[28], L. Christofek[77], T. Christoudias[43], S. Cihangir[50], D. Claes[67], J. Clutter[58], M. Cooke[50], W.E. Cooper[50], M. Corcoran[80], F. Couderc[18], M.-C. Cousinou[15], S. Crépé-Renaudin[14], V. Cuplov[59], D. Cutts[77], M. Ćwiok[30], H. da Motta[2], A. Das[45], G. Davies[43], K. De[78], S.J. de Jong[35], E. De La Cruz-Burelo[33], C. De Oliveira Martins[3], K. DeVaughan[67], J.D. Degenhardt[64], F. Déliot[18], M. Demarteau[50], R. Demina[71], D. Denisov[50], S.P. Denisov[39], S. Desai[50], H.T. Diehl[50], M. Diesburg[50], A. Dominguez[67], H. Dong[72], T. Dorland[82], A. Dubey[28], L.V. Dudko[38], L. Duflot[16], S.R. Dugad[29], D. Duggan[49], A. Duperrin[15], J. Dyer[65], A. Dyshkant[52], M. Eads[67], D. Edmunds[65], J. Ellison[48], V.D. Elvira[50], Y. Enari[77], S. Eno[61], P. Ermolov[38,‡], H. Evans[54], A. Evdokimov[73], V.N. Evdokimov[39], A.V. Ferapontov[59], T. Ferbel[71], F. Fiedler[24], F. Filthaut[35], W. Fisher[50], H.E. Fisk[50], M. Fortner[52], H. Fox[42], S. Fu[50], S. Fuess[50], T. Gadfort[70], C.F. Galea[35], C. Garcia[71], A. Garcia-Bellido[71], V. Gavrilov[37], P. Gay[13], W. Geist[19], W. Geng[15,65], C.E. Gerber[51], Y. Gershtein[49], D. Gillberg[6], G. Ginther[71], N. Gollub[41], B. Gómez[8], A. Goussiou[82], P.D. Grannis[72], H. Greenlee[50], Z.D. Greenwood[60], E.M. Gregores[4], G. Grenier[20], Ph. Gris[13], J.-F. Grivaz[16], A. Grohsjean[25], S. Grünendahl[50], M.W. Grünewald[30], F. Guo[72], J. Guo[72], G. Gutierrez[50], P. Gutierrez[75], A. Haas[70], N.J. Hadley[61], P. Haefner[25], S. Hagopian[49], J. Haley[68], I. Hall[65], R.E. Hall[47], L. Han[7], K. Harder[44], A. Harel[71], J.M. Hauptman[57], J. Hays[43], T. Hebbeker[21], D. Hedin[52], J.G. Hegeman[34], A.P. Heinson[48], U. Heintz[62], C. Hensel[22,d], K. Herner[72], G. Hesketh[63], M.D. Hildreth[55], R. Hirosky[81], J.D. Hobbs[72], B. Hoeneisen[12], H. Hoeth[26], M. Hohlfeld[22], S. Hossain[75], P. Houben[34], Y. Hu[72], Z. Hubacek[10], V. Hynek[9], I. Iashvili[69], R. Illingworth[50], A.S. Ito[50], S. Jabeen[62], M. Jaffré[16], S. Jain[75], K. Jakobs[23], C. Jarvis[61], R. Jesik[43], K. Johns[45], C. Johnson[70], M. Johnson[50], D. Johnston[67], A. Jonckheere[50], P. Jonsson[43], A. Juste[50], E. Kajfasz[15], J.M. Kalk[60], D. Karmanov[38], P.A. Kasper[50], I. Katsanos[70], D. Kau[49], V. Kaushik[78], R. Kehoe[79], S. Kermiche[15], N. Khalatyan[50], A. Khanov[76], A. Kharchilava[69], Y.M. Kharzheev[36], D. Khatidze[70], T.J. Kim[31], M.H. Kirby[53], M. Kirsch[21], B. Klima[50], J.M. Kohli[27], J.-P. Konrath[23], A.V. Kozelov[39], J. Kraus[65], T. Kuhl[24], A. Kumar[69], A. Kupco[11], T. Kurča[20], V.A. Kuzmin[38], J. Kvita[9], F. Lacroix[13], D. Lam[55], S. Lammers[70], G. Landsberg[77], P. Lebrun[20], W.M. Lee[50], A. Leflat[38], J. Lellouch[17], J. Li[78,‡], L. Li[48], Q.Z. Li[50], S.M. Lietti[5], J.K. Lim[31], J.G.R. Lima[52], D. Lincoln[50], J. Linnemann[65], V.V. Lipaev[39], R. Lipton[50], Y. Liu[7], Z. Liu[6], A. Lobodenko[40], M. Lokajicek[11], P. Love[42], H.J. Lubatti[82], R. Luna[3], A.L. Lyon[50], A.K.A. Maciel[2], D. Mackin[80], R.J. Madaras[46], P. Mättig[26], C. Magass[21], A. Magerkurth[64], P.K. Mal[82], H.B. Malbouisson[3], S. Malik[67], V.L. Malyshev[36], Y. Maravin[59], B. Martin[14], R. McCarthy[72], A. Melnitchouk[66], L. Mendoza[8], P.G. Mercadante[5], M. Merkin[38], K.W. Merritt[50], A. Meyer[21], J. Meyer[22,d], J. Mitrevski[70], R.K. Mommsen[44], N.K. Mondal[29], R.W. Moore[6], T. Moulik[58], G.S. Muanza[20], M. Mulhearn[70], O. Mundal[22], L. Mundim[3], E. Nagy[15], M. Naimuddin[50], M. Narain[77], N.A. Naumann[35], H.A. Neal[64], J.P. Negret[8], P. Neustroev[40], H. Nilsen[23], H. Nogima[3], S.F. Novaes[5], T. Nunnemann[25], V. O'Dell[50], D.C. O'Neil[6], G. Obrant[40], C. Ochando[16], D. Onoprienko[59], N. Oshima[50], N. Osman[43], J. Osta[55], R. Otec[10], G.J. Otero y Garzón[50], M. Owen[44], P. Padley[80], M. Pangilinan[77], N. Parashar[56], S.-J. Park[22,d], S.K. Park[31], J. Parsons[70], R. Partridge[77], N. Parua[54], A. Patwa[73], G. Pawloski[80], B. Penning[23], M. Perfilov[38], K. Peters[44], Y. Peters[26], P. Pétroff[16], M. Petteni[43], R. Piegaia[1],

J. Piper[65], M.-A. Pleier[22], P.L.M. Podesta-Lerma[33,c], V.M. Podstavkov[50], Y. Pogorelov[55], M.-E. Pol[2], P. Polozov[37], B.G. Pope[65], A.V. Popov[39], C. Potter[6], W.L. Prado da Silva[3], H.B. Prosper[49], S. Protopopescu[73], J. Qian[64], A. Quadt[22,d], B. Quinn[66], A. Rakitine[42], M.S. Rangel[2], K. Ranjan[28], P.N. Ratoff[42], P. Renkel[79], P. Rich[44], J. Rieger[54], M. Rijssenbeek[72], I. Ripp-Baudot[19], F. Rizatdinova[76], S. Robinson[43], R.F. Rodrigues[3], M. Rominsky[75], C. Royon[18], P. Rubinov[50], R. Ruchti[55], G. Safronov[37], G. Sajot[14], A. Sánchez-Hernández[33], M.P. Sanders[17], B. Sanghi[50], G. Savage[50], L. Sawyer[60], T. Scanlon[43], D. Schaile[25], R.D. Schamberger[72], Y. Scheglov[40], H. Schellman[53], T. Schliephake[26], S. Schlobohm[82], C. Schwanenberger[44], A. Schwartzman[68], R. Schwienhorst[65], J. Sekaric[49], H. Severini[75], E. Shabalina[51], M. Shamim[59], V. Shary[18], A.A. Shchukin[39], R.K. Shivpuri[28], V. Siccardi[19], V. Simak[10], V. Sirotenko[50], P. Skubic[75], P. Slattery[71], D. Smirnov[55], G.R. Snow[67], J. Snow[74], S. Snyder[73], S. Söldner-Rembold[44], L. Sonnenschein[17], A. Sopczak[42], M. Sosebee[78], K. Soustruznik[9], B. Spurlock[78], J. Stark[14], J. Steele[60], V. Stolin[37], D.A. Stoyanova[39], J. Strandberg[64], S. Strandberg[41], M.A. Strang[69], E. Strauss[72], M. Strauss[75], R. Ströhmer[25], D. Strom[53], L. Stutte[50], S. Sumowidagdo[49], P. Svoisky[55], A. Sznajder[3], P. Tamburello[45], A. Tanasijczuk[1], W. Taylor[6], B. Tiller[25], F. Tissandier[13], M. Titov[18], V.V. Tokmenin[36], I. Torchiani[23], D. Tsybychev[72], B. Tuchming[18], C. Tully[68], P.M. Tuts[70], R. Unalan[65], L. Uvarov[40], S. Uvarov[40], S. Uzunyan[52], B. Vachon[6], P.J. van den Berg[34], R. Van Kooten[54], W.M. van Leeuwen[34], N. Varelas[51], E.W. Varnes[45], I.A. Vasilyev[39], P. Verdier[20], L.S. Vertogradov[36], M. Verzocchi[50], D. Vilanova[18], F. Villeneuve-Seguier[43], P. Vint[43], P. Vokac[10], M. Voutilainen[67,e], R. Wagner[68], H.D. Wahl[49], M.H.L.S. Wang[50], J. Warchol[55], G. Watts[82], M. Wayne[55], G. Weber[24], M. Weber[50,f], L. Welty-Rieger[54], A. Wenger[23,g], N. Wermes[22], M. Wetstein[61], A. White[78], D. Wicke[26], M. Williams[42], G.W. Wilson[58], S.J. Wimpenny[48], M. Wobisch[60], D.R. Wood[63], T.R. Wyatt[44], Y. Xie[77], S. Yacoob[53], R. Yamada[50], W.-C. Yang[44], T. Yasuda[50], Y.A. Yatsunenko[36], H. Yin[7], K. Yip[73], H.D. Yoo[77], S.W. Youn[53], J. Yu[78], C. Zeitnitz[26], S. Zelitch[81], T. Zhao[82], B. Zhou[64], J. Zhu[72], M. Zielinski[71], D. Zieminska[54], A. Zieminski[54,‡], L. Zivkovic[70], V. Zutshi[52], and E.G. Zverev[38]

(The DØ Collaboration)

[1] *Universidad de Buenos Aires, Buenos Aires, Argentina*
[2] *LAFEX, Centro Brasileiro de Pesquisas Físicas, Rio de Janeiro, Brazil*
[3] *Universidade do Estado do Rio de Janeiro, Rio de Janeiro, Brazil*
[4] *Universidade Federal do ABC, Santo André, Brazil*
[5] *Instituto de Física Teórica, Universidade Estadual Paulista, São Paulo, Brazil*
[6] *University of Alberta, Edmonton, Alberta, Canada, Simon Fraser University, Burnaby, British Columbia, Canada, York University, Toronto, Ontario, Canada, and McGill University, Montreal, Quebec, Canada*
[7] *University of Science and Technology of China, Hefei, People's Republic of China*
[8] *Universidad de los Andes, Bogotá, Colombia*
[9] *Center for Particle Physics, Charles University, Prague, Czech Republic*
[10] *Czech Technical University, Prague, Czech Republic*
[11] *Center for Particle Physics, Institute of Physics, Academy of Sciences of the Czech Republic, Prague, Czech Republic*
[12] *Universidad San Francisco de Quito, Quito, Ecuador*
[13] *LPC, Université Blaise Pascal, CNRS/IN2P3, Clermont, France*
[14] *LPSC, Université Joseph Fourier Grenoble 1, CNRS/IN2P3, Institut National Polytechnique de Grenoble, Grenoble, France*
[15] *CPPM, Aix-Marseille Université, CNRS/IN2P3, Marseille, France*
[16] *LAL, Université Paris-Sud, IN2P3/CNRS, Orsay, France*
[17] *LPNHE, IN2P3/CNRS, Universités Paris VI and VII, Paris, France*
[18] *CEA, Irfu, SPP, Saclay, France*
[19] *IPHC, Université Louis Pasteur, CNRS/IN2P3, Strasbourg, France*
[20] *IPNL, Université Lyon 1, CNRS/IN2P3, Villeurbanne, France and Université de Lyon, Lyon, France*
[21] *III. Physikalisches Institut A, RWTH Aachen University, Aachen, Germany*
[22] *Physikalisches Institut, Universität Bonn, Bonn, Germany*
[23] *Physikalisches Institut, Universität Freiburg, Freiburg, Germany*
[24] *Institut für Physik, Universität Mainz, Mainz, Germany*
[25] *Ludwig-Maximilians-Universität München, München, Germany*
[26] *Fachbereich Physik, University of Wuppertal, Wuppertal, Germany*
[27] *Panjab University, Chandigarh, India*
[28] *Delhi University, Delhi, India*
[29] *Tata Institute of Fundamental Research, Mumbai, India*

[30] University College Dublin, Dublin, Ireland
[31] Korea Detector Laboratory, Korea University, Seoul, Korea
[32] SungKyunKwan University, Suwon, Korea
[33] CINVESTAV, Mexico City, Mexico
[34] FOM-Institute NIKHEF and University of Amsterdam/NIKHEF, Amsterdam, The Netherlands
[35] Radboud University Nijmegen/NIKHEF, Nijmegen, The Netherlands
[36] Joint Institute for Nuclear Research, Dubna, Russia
[37] Institute for Theoretical and Experimental Physics, Moscow, Russia
[38] Moscow State University, Moscow, Russia
[39] Institute for High Energy Physics, Protvino, Russia
[40] Petersburg Nuclear Physics Institute, St. Petersburg, Russia
[41] Lund University, Lund, Sweden, Royal Institute of Technology and Stockholm University, Stockholm, Sweden, and Uppsala University, Uppsala, Sweden
[42] Lancaster University, Lancaster, United Kingdom
[43] Imperial College, London, United Kingdom
[44] University of Manchester, Manchester, United Kingdom
[45] University of Arizona, Tucson, Arizona 85721, USA
[46] Lawrence Berkeley National Laboratory and University of California, Berkeley, California 94720, USA
[47] California State University, Fresno, California 93740, USA
[48] University of California, Riverside, California 92521, USA
[49] Florida State University, Tallahassee, Florida 32306, USA
[50] Fermi National Accelerator Laboratory, Batavia, Illinois 60510, USA
[51] University of Illinois at Chicago, Chicago, Illinois 60607, USA
[52] Northern Illinois University, DeKalb, Illinois 60115, USA
[53] Northwestern University, Evanston, Illinois 60208, USA
[54] Indiana University, Bloomington, Indiana 47405, USA
[55] University of Notre Dame, Notre Dame, Indiana 46556, USA
[56] Purdue University Calumet, Hammond, Indiana 46323, USA
[57] Iowa State University, Ames, Iowa 50011, USA
[58] University of Kansas, Lawrence, Kansas 66045, USA
[59] Kansas State University, Manhattan, Kansas 66506, USA
[60] Louisiana Tech University, Ruston, Louisiana 71272, USA
[61] University of Maryland, College Park, Maryland 20742, USA
[62] Boston University, Boston, Massachusetts 02215, USA
[63] Northeastern University, Boston, Massachusetts 02115, USA
[64] University of Michigan, Ann Arbor, Michigan 48109, USA
[65] Michigan State University, East Lansing, Michigan 48824, USA
[66] University of Mississippi, University, Mississippi 38677, USA
[67] University of Nebraska, Lincoln, Nebraska 68588, USA
[68] Princeton University, Princeton, New Jersey 08544, USA
[69] State University of New York, Buffalo, New York 14260, USA
[70] Columbia University, New York, New York 10027, USA
[71] University of Rochester, Rochester, New York 14627, USA
[72] State University of New York, Stony Brook, New York 11794, USA
[73] Brookhaven National Laboratory, Upton, New York 11973, USA
[74] Langston University, Langston, Oklahoma 73050, USA
[75] University of Oklahoma, Norman, Oklahoma 73019, USA
[76] Oklahoma State University, Stillwater, Oklahoma 74078, USA
[77] Brown University, Providence, Rhode Island 02912, USA
[78] University of Texas, Arlington, Texas 76019, USA
[79] Southern Methodist University, Dallas, Texas 75275, USA
[80] Rice University, Houston, Texas 77005, USA
[81] University of Virginia, Charlottesville, Virginia 22901, USA and
[82] University of Washington, Seattle, Washington 98195, USA

(Dated: August 8, 2008)

We report a search for the standard model Higgs boson in the missing energy and acoplanar b-jet topology, using an integrated luminosity of 0.93 fb^{-1} recorded by the D0 detector at the Fermilab Tevatron $p\overline{p}$ Collider. The analysis includes signal contributions from $p\overline{p} \to ZH \to \nu\overline{\nu}b\overline{b}$, as well as from WH production in which the charged lepton from the W boson decay is undetected. Neural networks are used to separate signal from background. In the absence of a signal, we set limits on $\sigma(p\overline{p} \to VH) \times B(H \to b\overline{b})$ at the 95% C.L. of 2.6 – 2.3 pb, for Higgs boson masses in the range 105 – 135 GeV, where $V = W, Z$. The corresponding expected limits range from 2.8 pb – 2.0 pb.

PACS numbers: 13.85.Qk, 13.85.Ni, 13.85.Rm

The Higgs mechanism, postulated to explain electroweak symmetry breaking, predicts the existence of the Higgs boson, which has yet to be found. The CERN e^+e^- Collider experiments placed a lower limit on its mass of 114.4 GeV at 95% C.L. [1]. Global fits to precision electroweak data suggest a mass of $M_H < 160$ GeV at 95% C.L. [2]. In this range, the Fermilab Tevatron $p\bar{p}$ Collider has significant discovery potential. Searches in the missing energy and acoplanar b-jet channel have been published by CDF [3] and D0 [4]. This channel is sensitive to ZH associated production when the Z decays to neutrinos and WH production when the charged lepton from the W decay is undetected. The result in this Letter supercedes our previous work. As well as benefitting from more data this analysis uses artificial neural networks (NN) for heavy flavor tagging (b tagging) and in event selection.

The D0 detector is described in Ref. [5]. Dedicated triggers selected events with acoplanar jets and large imbalance in transverse momentum, ($\not\!\!E_T$), as defined by energy deposited in the D0 calorimeters. After imposing data quality requirements the data correspond to an integrated luminosity of 0.93 fb^{-1} [6]. Time-dependent adjustments have been made to the trigger requirements to compensate for the increasing peak instantaneous luminosity of the Tevatron. The selection criteria therefore varied somewhat, but typically required $\not\!\!H_T > 30$ GeV (where $\not\!\!H_T$ is the imbalance in transverse momentum calculated using only well reconstructed jets) for jets reconstructed at the highest level trigger, and an azimuthal angle between the two leading (highest p_T) jets of $\Delta\phi(jet_1, jet_2) < 170°$.

Event selection requires at least two jets with $p_T > 20$ GeV, $|\eta| < 1.1$ (central calorimeter) or $1.4 < |\eta| < 2.5$ (end calorimeters) and $\Delta\phi(jet_1, jet_2) < 165°$, where η is the pseudorapidity measured from the center of the detector ($\eta = -\ln(\tan\frac{\theta}{2})$, where θ is the angle relative to the beam axis). Reconstructed jets are corrected based on the expected calorimeter response, energy lost due to showering out of the jet cone, and energy deposited in the jet cone not associated with the jet [7]. We require the distance along the beam axis of the primary vertex from the center of the detector (z_{PV}) to be less than 35 cm, and at least three tracks attached to the primary vertex to ensure b tagging capability. We also require $\not\!\!E_T > 50$ GeV and $H_T < 240$ GeV (where H_T is the scalar sum of the transverse momenta calculated using only well reconstructed jets) to reduce the contribution from $t\bar{t}$ background. A significant proportion of W/Z+jets events in which the bosons decay into charged leptons are rejected by vetoing isolated leptons (electrons or muons).

Signal samples of $ZH \to \nu\nu b\bar{b}$ and $WH \to \ell\nu_\ell b\bar{b}$ ($\ell = e, \mu, \tau$) were generated for $105 \le M_H \le 135$ GeV using PYTHIA [8]. There are two types of backgrounds: physical processes modelled by Monte Carlo (MC) generators and instrumental background predicted from data. ALPGEN [9] was used to simulate $t\bar{t}$ production with up to four jets. Samples of W+jets (W decays to all three lepton pairs for light jets jj, $b\bar{b}$ and $c\bar{c}$ jets) and Z+jets (including $Z \to \nu\overline{\nu}$ and $Z \to \tau^+\tau^-$ processes for jj, $b\bar{b}$ and $c\bar{c}$ jets) were also generated separately using ALPGEN. Diboson processes (WW, WZ and ZZ) were generated with PYTHIA. The samples generated with ALPGEN were processed through PYTHIA for showering and hadronization. Next-to-leading order (NLO) cross sections were used for normalizing all processes (NNLO for $t\bar{t}$). All samples were processed through the D0 detector simulation and the reconstruction software. The trigger requirements were modeled using a parametrized trigger simulation determined from data.

As b tagging is applied later, jets are required to be "taggable", i.e. satisfy certain minimal tracking and vertexing criteria; a jet must have at least two tracks, one with $p_T > 1$ and the other with > 0.5 GeV, each with ≥ 2 hits in the silicon vertex detector, and $\Delta\mathcal{R}(track, jet) < 0.5$, where $\Delta\mathcal{R} = \sqrt{(\Delta\phi)^2 + (\Delta\eta)^2}$, with ϕ being the azimuthal angle. The fraction of taggable jets was investigated as a function of p_T, η and z_{PV} using a W+jets data sample. Jets in the simulation are corrected by the ratio of taggabilities measured in data and in MC, which is found to depend only on η. Correction factors of 0.97 $\pm$ 0.01 and 0.95 $\pm$ 0.03 (statistical errors) are used for the central and end calorimeters, respectively.

For events originating from hard processes with genuine missing transverse energy, the $\not\!\!H_T$, $\not\!\!E_T$ and $\not\!\!T_T$ (where $\not\!\!T_T$ is the negative of the vector sum of the p_T of all tracks) point in the same direction and are correlated. However, dijet events in which one of the jets has been mismeasured typically have $\not\!\!E_T$ pointing along the direction of one of the jets. Instrumental effects produce events that tend to have $\not\!\!E_T$ and $\not\!\!T_T$ misaligned. To reduce instrumental background, we require:

- $\min\{\Delta\phi_i(\not\!\!E_T, \mathrm{jet}_i)\} > 0.15$, where $\min\{\Delta\phi_i(\not\!\!E_T, \mathrm{jet}_i)\}$ is the minimum of the difference in azimuthal angle between the direction of $\not\!\!E_T$ and any of the jets;
- $\not\!\!E_T(\mathrm{GeV}) > -40 \times \min\{\Delta\phi_i(\not\!\!E_T, \mathrm{jet}_i)\} + 80$;
- $\Delta\phi(\not\!\!E_T, \not\!\!T_T) < \pi/2$, where $\Delta\phi(\not\!\!E_T, \not\!\!T_T)$ is the difference in azimuthal angle between the directions of $\not\!\!E_T$ and $\not\!\!T_T$;
- $-0.1 < \mathcal{A}(\not\!\!E_T, \not\!\!H_T) < 0.2$, where $\mathcal{A}(\not\!\!E_T, \not\!\!H_T) \equiv (\not\!\!E_T - \not\!\!H_T)/(\not\!\!E_T + \not\!\!H_T)$ is the asymmetry between $\not\!\!E_T$ and $\not\!\!H_T$.

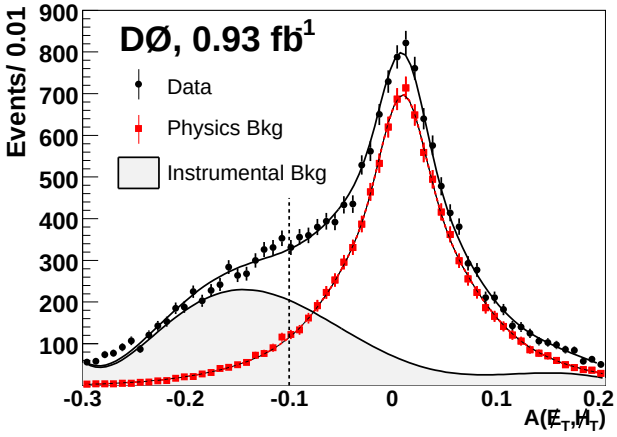

FIG. 1: $\mathcal{A}(\not\!\!E_T, \not\!\!H_T)$ for data, MC physics background and instrumental background in the signal region, before implementing b tagging. The final selection corresponds to $-0.1 < \mathcal{A}(\not\!\!E_T, \not\!\!H_T) < 0.2$.

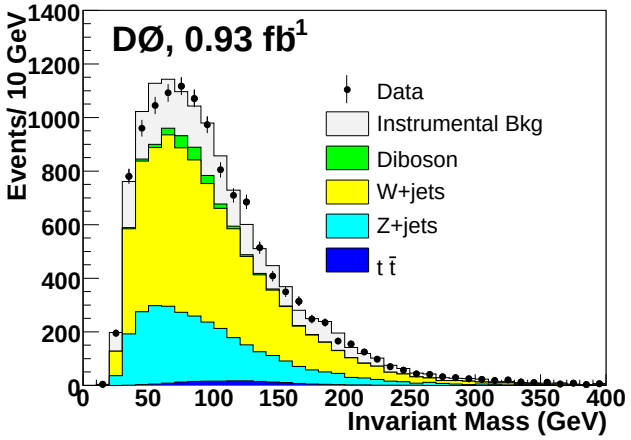

FIG. 2: Invariant mass distribution of the two leading jets before b tagging requirements.

The residual contribution of the instrumental background is determined from distributions in $\mathcal{A}(\not\!\!E_T, \not\!\!H_T)$ and $\Delta\phi(\not\!\!E_T, \not\!\!T_T)$. The instrumental background peaks at $\mathcal{A}(\not\!\!E_T, \not\!\!H_T) < 0$ because it is dominated by poor quality jets that are taken into account when calculating $\not\!\!E_T$ but not $\not\!\!H_T$. Signal and sideband regions are defined as having $\Delta\phi(\not\!\!E_T, \not\!\!T_T) < \pi/2$ and $\Delta\phi(\not\!\!E_T, \not\!\!T_T) > \pi/2$, respectively. The shape of the backgrounds from simulated processes, for both regions, are taken directly from the MC. We fit a sixth-order polynomial to the $\mathcal{A}(\not\!\!E_T, \not\!\!H_T)$ distribution in the sideband region to determine the shape (before b-jet tagging) for the instrumental background (after subtracting the MC background contribution) and a triple Gaussian for the signal region. We then do a combined physics and instrumental backgrounds fit to data in the signal region, as shown in Fig. 1. For this combined fit, the simulation and instrumental background shapes are fixed to those from previous fits, and only the absolute scale of the two types of background is allowed to float. The normalization of the background for simulated (MC) processes is found to be 1.06 ± 0.02 (statistical error), in good agreement with the expected cross sections. The invariant mass distribution of the two leading jets after final background normalization is shown in Fig. 2.

The standard D0 neural network b tagging algorithm employs lifetime based information involving track impact parameters and secondary vertices [10]. We optimize the choice of b tagging operating points for best signal significance and require one tight b-tag (b-tag efficiency $\sim$50% for a mistag rate of $\sim$0.4%) and one loose b-tag (b-tag efficiency $\sim$70% for a mistag rate of $\sim$4.5%). Table I shows the number of expected events from MC and instrumental backgrounds along with the number of events observed in data, before and after b tagging. After b tagging, 134 ± 18 events are expected and 140 are observed.

TABLE I: Number of events after selections.

Sample	No b-tag	Double b-tag
$ZH(M_H = 115\ GeV)$	2.46 ± 0.34	0.88 ± 0.12
$WH(M_H = 115\ GeV)$	1.75 ± 0.25	0.61 ± 0.08
Wjj	5180 ± 670	7.6 ± 1.4
$Wb\bar{b}$	397 ± 52	35.4 ± 7.1
$Wc\bar{c}$	1170 ± 150	9.3 ± 1.9
$Z(\rightarrow \tau^+\tau^-)jj$	107 ± 14	0.25 ± 0.05
$Z(\rightarrow \nu\overline{\nu})jj$	2130 ± 280	0.63 ± 0.12
$Z(\rightarrow \tau^+\tau^-)b\bar{b}$	6.39 ± 0.83	0.63 ± 0.13
$Z(\rightarrow \nu\overline{\nu})b\bar{b}$	229 ± 30	24.9 ± 5.0
$Z(\rightarrow \tau^+\tau^-)c\bar{c}$	12.8 ± 1.7	0.18 ± 0.04
$Z(\rightarrow \nu\overline{\nu})c\bar{c}$	467 ± 61	4.9 ± 1.0
$t\bar{t}$	172 ± 34	29.1 ± 6.1
Diboson	228 ± 25	3.84 ± 0.50
Total MC Bkg	10100 ± 800	117 ± 17
Instrumental Bkg	2560 ± 330	17.2 ± 3.4
Total Bkg	12700 ± 900	134 ± 18
Observed Events	12500	140

Further signal-to-background discrimination is achieved by combining several kinematic variables using a NN. Independent MC samples are used for NN training, NN testing and limit setting. The instrumental background contribution is not taken into account during training, as its inclusion does not improve the expected sensitivity. The signal sample used for training is a combination of the ZH and WH contributions. Events are weighted such that the total contribution from each sample is that expected after b tagging. The NN input variables are the invariant mass of the two leading jets in the event, $\Delta\mathcal{R}$ between the two jets, p_T of the leading jet, p_T of the next-to-leading jet, $\not\!\!E_T$, $\not\!\!H_T$ and H_T. The input variables are selected for their ability to separate signal and background and to provide good modeling of data. The NN outputs for signal, background and data

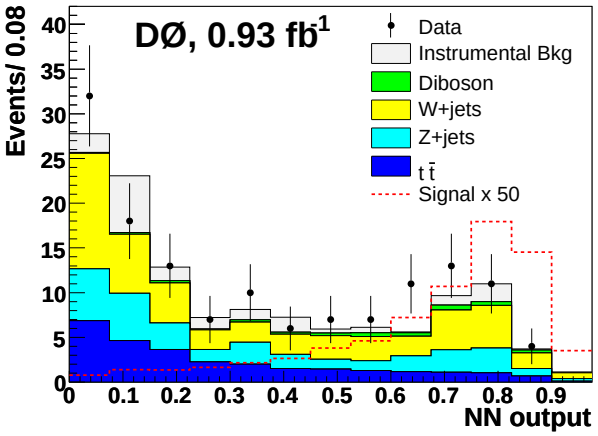

FIG. 3: NN output distributions for $M_H = 115$ GeV after b tagging. The MC expectation for the Higgs signal is scaled up by a factor of 50.

are shown in Fig. 3.

Systematic uncertainties affect the expected number of signal and background events ("overall uncertainties") as well as the shape of the distribution in the NN output ("differential uncertainties"). We estimate overall systematic uncertainties associated with luminosity (6.1%), trigger efficiencies (5%), jet identification (5%), b tagging (7%), background MC cross section (6-18%) and instrumental background (20%). All systematic uncertainties are common and correlated between signal and backgrounds, except for the uncertainties on the cross sections and the instrumental background. Differential uncertainties are estimated from the difference in the shape of the NN output by varying the jet energy scale (JES) by its uncertainties in a correlated way for all signal and background MC samples at each mass point. The difference in the distribution of the NN output from the uncertainty in the shape of the MC di-b-jet mass spectrum is also taken into account at each M_H point. The JES uncertainty was estimated to be $\leq 10\%$ and that for the mass spectrum $\leq 8\%$. Additionally, the impact on the NN output of the possible discrepancy in the low mass region in Fig. 2 was investigated and found to be negligible.

We set a limit on the Higgs production cross section using a modified frequentist approach with a Poisson log-likelihood ratio (LLR) statistic [11, 12]. The NN distribution is used to construct the LLR test statistic. The impact of systematic uncertainties is incorporated through "marginalization" of the Poisson probability distributions for signal and background, assuming Gaussian distributions. We adjust each component of systematic uncertainty by introducing nuisance multipliers for each and maximizing the likelihood for the agreement between prediction and data with respect to the nuisance parameters, constrained by the prior Gaussian uncertainties for each. All correlations in the systematics are maintained between signal and background. The resulting limits are presented in Table II.

TABLE II: Expected (Exp.) and observed (Obs.) limits in pb and as a ratio to the SM Higgs cross section (in parentheses), assuming $H \to b\bar{b}$.

Higgs Mass (GeV)	105	115	125	135
ZH Exp.	1.6 (15)	1.5 (19)	1.4 (29)	1.2 (47)
ZH Obs.	1.5 (14)	1.5 (20)	1.4 (30)	1.3 (51)
WH Exp.	4.8 (25)	4.3 (33)	3.8 (47)	3.6 (84)
WH Obs.	4.4 (23)	5.0 (39)	4.4 (55)	4.2 (99)
VH Exp.	2.8 (9.1)	2.5 (12)	2.3 (18)	2.0 (30)
VH Obs.	2.6 (8.7)	2.7 (13)	2.5 (20)	2.3 (34)

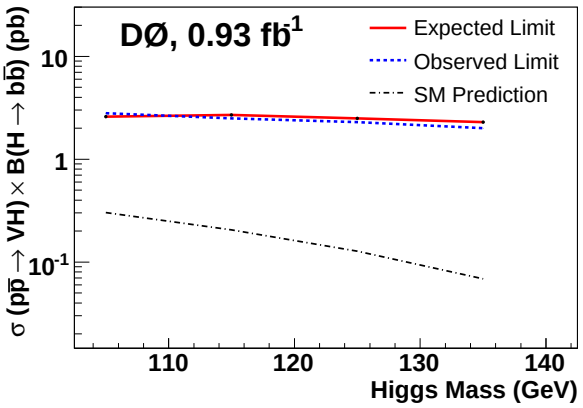

FIG. 4: 95 % C.L. upper limit on $\sigma(p\overline{p} \to VH) \times B(H \to b\overline{b})$ (and corresponding expected limit) for VH production vs. Higgs mass.

In summary, we have performed a search for the standard model Higgs produced in association with either a Z or W boson (denoted as VH), in the final state topology requiring missing transverse momentum and two b-tagged jets in 0.93 fb^{-1} of data. In the absence of a significant excess in data above background expectation, we set limits on $\sigma(p\overline{p} \to VH) \times B(H \to b\overline{b})$ at the 95% confidence level of 2.6 pb – 2.3 pb for Higgs boson masses in the range 105 – 135 GeV. The corresponding expected limits range from 2.8 pb – 2.0 pb. The expected and observed limits, along with the SM prediction, are shown in Fig. 4 as a function of Higgs mass. This is the most stringent limit to date in this channel at a hadron collider.

We thank the staffs at Fermilab and collaborating institutions, and acknowledge support from the DOE and NSF (USA); CEA and CNRS/IN2P3 (France); FASI, Rosatom and RFBR (Russia); CNPq, FAPERJ, FAPESP and FUNDUNESP (Brazil); DAE and DST (India); Colciencias (Colombia); CONACyT (Mexico); KRF and KOSEF (Korea); CONICET and UBACyT (Argentina); FOM (The Netherlands); STFC (United Kingdom); MSMT and GACR (Czech Republic); CRC

Program, CFI, NSERC and WestGrid Project (Canada); BMBF and DFG (Germany); SFI (Ireland); The Swedish Research Council (Sweden); CAS and CNSF (China); and the Alexander von Humboldt Foundation (Germany).

[a] Visitor from Augustana College, Sioux Falls, SD, USA.
[b] Visitor from The University of Liverpool, Liverpool, UK.
[c] Visitor from ECFM, Universidad Autonoma de Sinaloa, Culiacán, Mexico.
[d] Visitor from II. Physikalisches Institut, Georg-August-University, Göttingen, Germany.
[e] Visitor from Helsinki Institute of Physics, Helsinki, Finland.
[f] Visitor from Universität Bern, Bern, Switzerland.
[g] Visitor from Universität Zürich, Zürich, Switzerland.
[‡] Deceased.

[1] LEP Collaborations, Phys. Lett. B **565**, 61 (2003).
[2] LEP electroweak working group, http://lepewwg.web.cern.ch/LEPEWWG/.
[3] T. Aaltonen *et al.* (CDF Collaboration), Phys. Rev. Lett. **100**, 211801 (2008).
[4] V.M. Abazov *et al.* (D0 Collaboration), Phys. Rev. Lett. **97**, 161803 (2006).
[5] V.M. Abazov *et al.* (D0 Collaboration), Nucl. Instrum. Methods Phys. Res. A **565**, 463 (2006).
[6] T. Andeen *et al.*, FERMILAB-TM-2365 (2007).
[7] V.M. Abazov *et al.* (D0 Collaboration), arXiv:0802.2400 [hep-ex] (2008), accepted by Phys. Rev. Lett.
[8] T. Sjöstrand *et al.*, arXiv:hep-ph/0308153 (2003). We used PYTHIA version 6.323.
[9] M. L. Mangano *et al.*, arXiv:hep-ph/0206293 (2003). We used ALPGEN version 2.05.
[10] T. Scanlon, FERMILAB-THESIS-2006-43 (2006).
[11] T. Junk, Nucl. Instrum. Methods Phys. Res. A **434**, 435 (1999).
[12] W. Fisher, FERMILAB-TM-2386-E (2007).